Role of Hot-Electron Preheating in the Compression of Direct-Drive Imploding Targets with Cryogenic D_2 Ablators

V. A. Smalyuk, D. Shvarts,* R. Betti,† J. A. Delettrez, D. H. Edgell, V. Yu. Glebov, V. N. Goncharov, R. L. McCrory,† D. D. Meyerhofer,† P. B. Radha, S. P. Regan, T. C. Sangster, W. Seka, S. Skupsky, C. Stoeckl, and B. Yaakobi
Laboratory for Laser Energetics, University of Rochester, 250 East River Road, Rochester, New York 14623-1299, USA

J. A. Frenje, C. K. Li, R. D. Petrasso,‡ and F. H. Séguin
Plasma Science and Fusion Center, Massachusetts Institute of Technology, Cambridge, Massachusetts 02139, USA
(Received 9 November 2007; published 8 May 2008)

The compression of direct-drive, spherical implosions is studied using cryogenic D_2 targets on the 60-beam, 351-nm OMEGA laser with intensities ranging from $\sim 3 \times 10^{14}$ to $\sim 1 \times 10^{15}$ W/cm^2. The hard-x-ray signal from hot electrons generated by laser-plasma instabilities increases with laser intensity, while the areal density decreases. Mitigating hot-electron production, by reducing the laser intensity to $\sim 3 \times 10^{14}$ W/cm^2, results in areal density of the order of ~ 140 mg/cm^2, in good agreement with 1D simulations. These results will be considered in future direct-drive-ignition designs.

DOI: 10.1103/PhysRevLett.100.185005 PACS numbers: 52.38.Dx

In direct-drive inertial confinement fusion (ICF) [1,2], a spherical target is irradiated directly by overlapped laser beams to achieve high compression of the fuel and a high temperature of the hot spot to trigger ignition and maximize the thermonuclear energy gain. The baseline direct-drive-ignition target design [3] for the National Ignition Facility (NIF) [2] uses cryogenic deuterium-tritium (DT) shells imploded with a total energy up to 1.5 MJ. To achieve a gain of ~40–50 will require a total target areal density (or ρR), at peak compression, of ~ 1500 mg/cm^2. A major goal of the current experimental campaign [4,5] on OMEGA is to demonstrate that high compression (i.e., high ρR) can be achieved in cryogenic D_2 implosions. Since the ρR is proportional to $E_L^{1/3}$ (E_L is the laser energy) [6], the peak areal density of 1500 mg/cm^2 at NIF energies ($E_L = 1.5$ MJ) is scaled to ~330 mg/cm^2 for OMEGA-size targets ($E_L \sim 16$ kJ). To achieve high compression, the shell entropy must be kept low. The entropy is defined [6] through $\alpha = [P(\mathrm{Mb})]/2.2[\rho(\mathrm{g/cm^3})]^{5/3}$ which, for a DT target, represents the adiabat or the ratio of the plasma pressure to the Fermi pressure of a fully degenerate electron gas [6]. As shown in Ref. [6], $\rho R(\mathrm{mg/cm^2}) \approx 2600[E_L(\mathrm{MJ})]^{1/3}\alpha^{-0.6}$ and high areal densities require low-adiabat ($\alpha \sim 2$–3) implosions to minimize the laser energy. Current direct-drive-ignition target designs [3] use DT as both the nuclear fuel and the ablator material. The DT ablator minimizes the hydrodynamic instability of the shell, because of its low-density and high-ablation velocity. This Letter shows that heating by the long mean free path, hot electrons ($T_{\mathrm{hot}} \sim 100$ keV) produced by the two-plasmon-decay (TPD) instability [7] in the hydrogenic coronal plasma is correlated with a significant increase in the shell adiabat. This result is of great importance to direct-drive ICF and will be considered in ignition target designs for the NIF.

TPD and resonance absorption (RA) can generate copious amounts of hot electrons as has been observed since the early stages of the ICF program when long-wavelength ($\lambda_L = 10$ μm) CO_2 lasers, and later glass ($\lambda_L = 1$ μm) lasers [2,7], were widely used. Since RA and TPD intensity thresholds increase as the laser wavelength is reduced, lasers in the UV range ($\lambda_L = 0.35$ and 0.25 μm) [7] have been adopted as the drivers of choice for ICF research. Since the TPD instability produces high-energy electrons even at UV laser frequencies (~ 100 keV electrons from TPD compared to ~10 keV from RA, under the conditions of the present OMEGA experiments) [7] it must be minimized to avoid target preheating. A very modest preheating of the shell causes a significant degradation of the implosion performance (a deposited preheating energy of 30 J increases the adiabat from 2 to 4 for OMEGA-scale targets). It is important to determine the constraints on the laser intensity required to prevent preheating effects in UV laser-driven implosions. The results of recent cryogenic implosions [5], performed using D_2 ablators with high-peak-intensity laser pulses of $\sim 10^{15}$ W/cm^2, showed that as the 1D adiabat of the fuel decreases, the achieved areal densities did not rise as expected, saturating at ~100 mg/cm^2, a degradation of up to a factor of 2 from 1D predictions. This Letter presents results of low-adiabat ($\alpha \sim 2$–3) cryogenic D_2 implosions with <5 μm thick deuterated plastic (CD) outer shells in which peak intensity was varied in the range from $\sim 3 \times 10^{14}$ to $\sim 1 \times 10^{15}$ W/cm^2. It shows a correlation between the TPD hot-electron x-ray signal and the target compression. For laser intensities above 3×10^{14} W/cm^2, the cryogenic shell compression is significantly less than 1D predictions,

potentially requiring preheating mitigation on NIF target designs.

Direct-drive implosions of ~860-μm, initial-diameter targets with shells consisting of a ~95-μm-thick inner D_2 ice layer and an outer 4-μm-thick plastic CD layer were carried out using the 351-nm, 60-beam OMEGA Laser System [8]. The targets were imploded with shaped, high-compression pulses in the range of intensities from $\sim 3 \times 10^{14}$ to $\sim 1 \times 10^{15}$ W/cm^2. The on-target energy was varied from ~13 kJ (in low-intensity implosions) to ~24 kJ (in high-intensity implosions). The results shown in this Letter include all OMEGA thin CD shell (< 5 μm) cryogenic implosions performed at low adiabat (in the range from ~2–3) that produced measurable areal-density and hot-electron x-ray signals. All experiments used standard OMEGA laser-beam-smoothing techniques including distributed phase plates [9], 1-THz 2D smoothing by spectral dispersion [10], and polarization smoothing [11], using birefringent wedges. The predicted areal densities, based on the 1D hydrodynamic code LILAC [12], including radiation transport, were in the range from ~140 to ~200 mg/cm^2. The 1D simulations used flux limited [13] and nonlocal (including resonant absorption) electron heat transport [14].

The hard-x-ray (HXR) signals (with photon energies of >40 keV) generated by hot electrons from the TPD instability were measured by the HXR detector [15]. The HXR detector has four channels measuring x rays >20, >40, >60, and >80 keV, respectively. Figure 1(a) shows signals measured by the >40 keV channel of this detector as a function of on-target peak laser intensity with the inferred hot-electron temperatures shown in Fig. 1(b). The hot-electron temperature was determined by fitting measured (by the four channels) signals assuming exponentially decaying hard-x-ray spectrum. The signal rises steeply with intensity in the range from $\sim 3 \times 10^{14}$ to $\sim 5 \times 10^{14}$ W/cm^2 and starts to saturate at $\sim 5 \times 10^{14}$ W/cm^2. The hot-electron temperature monotonically increases from 50 to 150 keV in this range of intensities. The electron stopping distance is greater than the target thickness during the laser pulse at these temperatures. This would lead to an almost uniform preheating of the target. In this work, a correlation between the hard-x-ray levels and areal-density degradation suggests that preheating due to energetic electrons is affecting target performance. The relationship between the x-ray signals and target preheating is still under study.

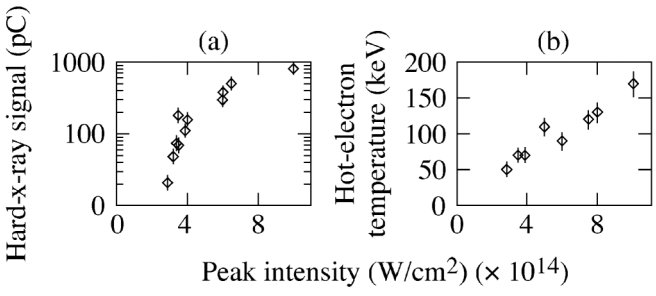

FIG. 1. (a) Measured hard-x-ray signal with photon energies >40 keV and (b) hot-electron temperature as a function of on-target peak laser intensity.

The HXR signal occurs during the last ~400 ps of the laser drive and is correlated with the observation of $3/2\omega$ scattered light, a typical signature of the TPD [15,16]. At this stage of the laser pulse, the corona consists mostly of deuterium plasma, where the TPD develops [16–18]. For these implosions, the measured burn-averaged areal density (inferred from the spectra of secondary protons [19] created near peak burn) is shown by diamonds in Fig. 2(a) as a function of the peak laser intensity. As the HXR signals and hot-electron temperature increase with the laser intensity, the areal density decreases. In these implosions, the predicted burn-averaged areal density varies in the range from ~140 to ~200 mg/cm^2. Figure 2(b) shows the dependence of the measured areal density normalized to the 1D code prediction with local electron transport (using a constant flux limiter of 0.06 [13]) as a function of the peak laser intensity [using the same data as in Fig. 2(a)] shown as diamonds. The simulation predictions including nonlocal electron transport [14] are shown by the circles. The nonlocal model more accurately describes the thermal electron transport at the ablation surface and, therefore, the laser absorption, shock strengths, and timing throughout the implosion [14]. The areal density and the normalized areal density (both local and nonlocal) decrease significantly for peak laser intensities above 3×10^{14} W/cm^2. This degradation correlates with the increase of the HXR signals [Fig. 1(a)]. The highest compression in low-adiabat implosions was achieved at the lowest intensities, when the HXR signals and associated fast-electron preheating were low, and the sensitivity of the implosion to nonlocal effects is minimal. The good performance at low intensities suggests that the physics governing temperature-density conditions of the fuel, such as fuel equation of state, opacity, shock propagation, and timing, are well described by the 1D code. These considerations

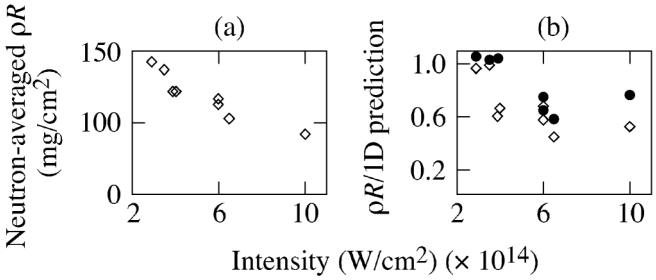

FIG. 2. (a) Peak-burn areal density, measured from secondary proton spectra, as a function of peak intensity. (b) Areal density divided by the 1D prediction as a function of peak intensity for the local model with a flux limiter of 0.06 (diamonds) and for the nonlocal model (circles).

and the intensity scaling of the HXR signal suggest that the areal-density degradation at high intensities is due to the hot-electron preheating.

A simple estimate of the areal-density degradation $\rho R_{\mathrm{exp}}/\rho R_{\mathrm{1D}}$ of the cold shell due to a preheating energy H_s can be carried out assuming a fully ionized, ideal plasma equation of state, with plasma density ρ proportional to the plasma pressure P and inversely proportional to the plasma temperature T; $\rho = AP/T$, where $A = m_i/(1+Z)$, m_i is the deuterium mass, and Z is its charge. The areal density depends [16] on laser energy E_L and shell adiabat as $\rho R \sim E_L^{1/3}/\alpha^{0.57}$. Since $\alpha \sim P/\rho^{5/3}$, the areal density is inversely proportional to the cold-shell temperature T_0,

$$\rho R_{\mathrm{exp}}/\rho R_{\mathrm{1D}} = T_0/(T_0 + \Delta T) = 1/(1 + \Delta T/T_0),$$

where ΔT is the temperature increase due to preheating. Assuming the deposited preheating energy increases the internal energy of the shell, $H_s = 3/2\Delta(PV)$, the temperature increase can be expressed through the preheating energy (using the ideal-gas equation of state) as $\Delta T = 2/3AH_s/M_s$, where the mass of the shell is $M_s = \rho V$. Using the following relationships [6], $P(\mathrm{Mb}) = 2.2\alpha[\rho(\mathrm{g/cm^3})]^{5/3}$ and $P(\mathrm{Mb}) = 120(I_{15})^{2/3}$, where I_{15} is the laser intensity in units of 10^{15} W/cm^2, the areal-density degradation can be expressed as

$$\rho R_{\mathrm{exp}}/\rho R_{\mathrm{1D}} \approx 1/[1 + 0.012H_s/(\xi_s \alpha^{3/5} I_{15}^{4/15})], \quad (1)$$

where $\xi_s = M_s/M_0$ is the fraction of the shell mass left after the ablation phase is divided by the nominal initial target mass (initial shell mass was $M_0 = 5 \times 10^{-5}$ g and $\xi_s \sim 0.5$ from 1D simulations). Figure 3 shows the estimated preheating energy H_s (circles) necessary to degrade compression performance [as shown in Fig. 2(b)], based on Eq. (1), where α was taken from 1D nonlocal simulations. The compressed-shell preheating energy necessary to significantly degrade compression performance is of the order of ~40 J. At the laser-drive energies of ~20 kJ, this preheating energy would correspond to ~0.2% of the drive energy if it were the sole explanation of areal degradation, a level of concern for direct-drive-ignition designs for NIF [20].

The correlation of the hot-electron x-ray signals with areal-density degradation does not preclude other sources, for example, uncertainties in the shock- and compression-wave modeling, hydrodynamic instabilities, areal-density sampling by diagnostic secondary protons, and preheating due to nonlocal electrons and x rays, currently under investigation. Since the laser pulse shapes are similar at the beginning of the drive (during a picket and a foot) for all implosions, the effects of pulse-shape contrast are similar for all implosions, and therefore, the pulse-shape contrast can be ruled out as a source of preheating.

The HXR signals depend on laser-drive intensity, the pulse shape, and ablator material. Figure 4 shows the dependence of the ratio of the HXR signal to the laser-drive energy as a function of the TPD threshold parameter [21] $\eta = [I_{14}L]/[230T_e]$, where I_{14} is laser intensity in units of 10^{14} W/cm^2, L is plasma density scale length in microns, and T_e is corona electron temperature in kilo-electron-volts [21]. The normalized hard-x-ray signal increases with the TPD parameter η. While in present OMEGA implosions η is below ~2.5, it increases to $\eta \sim 4$ in direct-drive-ignition designs for NIF, possibly

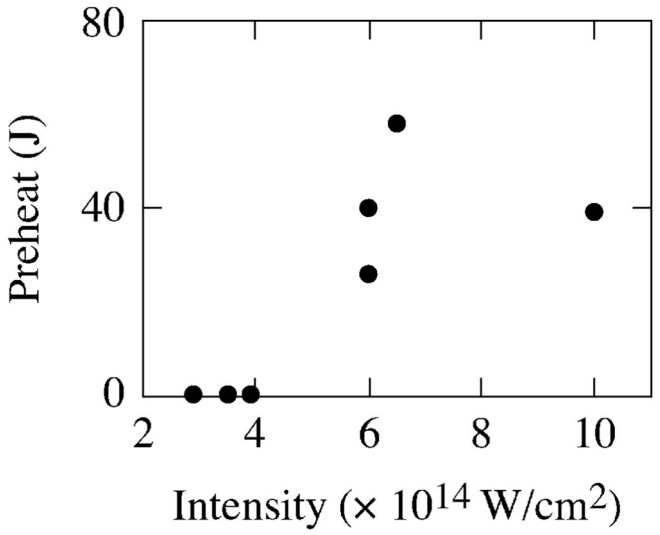

FIG. 3. Calculated preheating energy of the cold shell, required to explain the areal-density degradation (based on the nonlocal model), as a function of peak intensity.

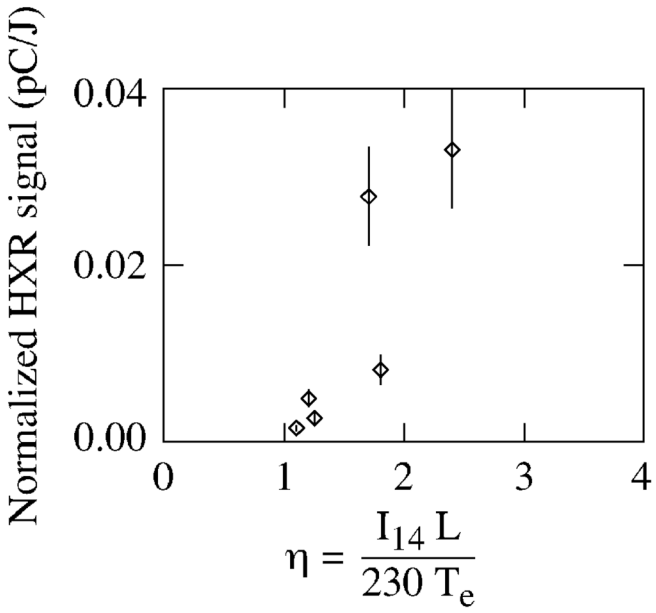

FIG. 4. Measured preheating x-ray emission divided by the total laser-drive energy as a function of the TPD threshold parameter $\eta = [I_{14}L]/[230T_e]$.

making targets more vulnerable to preheating. As a result, future direct-drive-ignition designs will consider techniques for hot-electron preheating mitigation. One of the examples of such mitigation was demonstrated in recent cryogenic implosions with all-plastic ablators [22]. While the hard-x-ray signals were reduced below detection levels in these experiments, the record areal densities of ~ 200 mg/cm^2 were achieved at relatively high drive intensity of $\sim 5 \times 10^{14}$ W/cm^2 [18,22].

In conclusion, hot electrons generated by TPD instability appear to play an important role in the compression degradation of low-adiabat cryogenic D_2 implosions. The compression degradation strongly correlates with the HXR signals that increase with laser intensity. The highest compression with areal densities of ~ 140 mg/cm^2 was achieved at a low peak laser intensity of $\sim 3 \times 10^{14}$ W/cm^2, where the TPD fast-electron x-ray generation is small. With such low intensity, it will be difficult to reach ignition-relevant implosion velocities ($\sim 3.5 \times 10^7$ cm/s). The direct-drive-ignition target designs for the NIF will consider techniques to reduce hot-electron preheating, including all-plastic ablators [18,22].

This work was supported by the U.S. Department of Energy Office of Inertial Confinement Fusion under Cooperative Agreement No. DE-FC52-08NA28302, the University of Rochester, and the New York State Energy Research and Development Authority.

*Also at: Nuclear Research Center Negev, Israel.
†Also at: Departments of Mechanical Engineering and Physics & Astronomy, University of Rochester, Rochester, NY, USA.
‡Visiting Senior Scientist, Laboratory for Laser Energetics, University of Rochester, Rochester, NY, USA.

[1] S. Atzeni and J. Meyer-ter-Vehn, *The Physics of Inertial Fusion: Beam Plasma Interaction, Hydrodynamics, Hot Dense Matter*, International Series of Monographs on Physics (Clarendon, Oxford, 2004).
[2] J. D. Lindl, *Inertial Confinement Fusion: The Quest for Ignition and Energy Gain Using Indirect Drive* (Springer-Verlag, New York, 1998).
[3] P. W. McKenty *et al.*, Phys. Plasmas **8**, 2315 (2001).
[4] T. C. Sangster *et al.*, Phys. Plasmas **14**, 058101 (2007).
[5] F. J. Marshall *et al.*, Phys. Plasmas **12**, 056302 (2005).
[6] C. D. Zhou and R. Betti, Phys. Plasmas **14**, 072703 (2007).
[7] W. L. Kruer, *The Physics of Laser-Plasma Interactions*, edited by D. Pines, Frontiers in Physics Vol. 73 (Addison-Wesley, Redwood City, CA, 1988).
[8] T. R. Boehly *et al.*, Opt. Commun. **133**, 495 (1997).
[9] Y. Lin, T. J. Kessler, and G. N. Lawrence, Opt. Lett. **20**, 764 (1995).
[10] S. P. Regan *et al.*, J. Opt. Soc. Am. B **17**, 1483 (2000).
[11] T. R. Boehly *et al.*, J. Appl. Phys. **85**, 3444 (1999).
[12] J. Delettrez *et al.*, Phys. Rev. A **36**, 3926 (1987).
[13] R. C. Malone, R. L. McCrory, and R. L. Morse, Phys. Rev. Lett. **34**, 721 (1975).
[14] V. N. Goncharov *et al.*, Phys. Plasmas **13**, 012702 (2006).
[15] C. Stoeckl *et al.*, Phys. Rev. Lett. **90**, 235002 (2003).
[16] W. Seka *et al.*, Phys. Plasmas **15**, 056312 (2008).
[17] V. N. Goncharov *et al.*, Phys. Plasmas **15**, 056310 (2008).
[18] R. McCrory *et al.*, Phys. Plasmas **15**, 055503 (2008).
[19] F. H. Séguin *et al.*, Rev. Sci. Instrum. **74**, 975 (2003).
[20] B. Yaakobi *et al.*, Phys. Plasmas **12**, 062703 (2005).
[21] A. Simon *et al.*, Phys. Fluids **26**, 3107 (1983).
[22] T. C. Sangster *et al.*, following Letter, Phys. Rev. Lett., **100**, 185006 (2008).